LEADER-BASED MULTIFRACTAL ANALYSIS FOR EVI fMRI TIME SERIES: ONGOING *vs* TASK-RELATED BRAIN ACTIVITY

Philippe Ciuciu[(1,2)]*, Patrice Abry*[(3)]*, Cécile Rabrait*[(1,2)]*, Herwig Wendt*[(3)] *and Alexis Roche*[(1,2)]

[(1)] NeuroSpin, CEA Saclay, Bâtiment 145, 91191 Gif-sur-Yvette, cedex France
[(2)] IFR 49, Functional neuroimaging institute, Paris, France
[(3)] CNRS, UMR 5672, Laboratoire de Physique. ENS Lyon, France.
[1] firstname.lastname@cea.fr, [3] firstname.lastname@ens-lyon.fr

ABSTRACT

Classical within-subject analysis in functional Magnetic Resonance Imaging (fMRI) relies on a detection step to localize which parts of the brain are activated by a given stimulus type. This is usually achieved using model-based approaches. Here, we propose an alternative exploratory scaling analysis. By nature, scaling analysis requires the use of long enough signals, with high frequency sampling rates. Recently, 3D Echo Volumar Imaging (EVI) techniques have emerged in fMRI allowing the very fast acquisition of successive brain volumes. The originality of this contribution is twofold: A new scaling analysis based on multifractal models instead of self-similarity ones and on wavelet Leaders instead of wavelet coefficients is introduced ; It is applied to high temporal resolution EVI data acquired both in resting state and during a visual paradigm. We estimate voxel-based multifractal attributes for both kinds of data and bring evidence confirming the existence of true scaling as opposed to superimposed non stationaries. Also, combining these estimates together with paired statistical tests, we observe significant scaling parameter changes between ongoing and evoked brain activity, which clearly validate an increase in long memory and suggest a global multifractality decrease effect.

***Index Terms*—** Biomedical signal detection, Magnetic resonance imaging, Multifractal analysis, Wavelet Leaders.

1. MOTIVATION: SCALING IN fMRI

Within-subject analysis in fMRI aims at detecting and localizing specific brain regions involved in the performance of cognitive or behavioral tasks. Classical approaches assume a linear and time-invariant relationship between the fMRI signals and the experimental design and rely therefore on a General Linear Model (GLM) and statistical tests to achieve this goal. fMRI time series are known to have a colored noise structure, the majority of which occurs at low frequency. Preliminary evidence that fMRI time series have long memory in time or $1/f$ spectral properties has been demonstrated on "resting state" motion-corrected datasets [1, 2]. Previous studies had shown that head movement is a common source of long memory noise caused by slow rotation or translation of subject's head through an imperfectly homogeneous magnetic field. Physiological factors such as cardiac beat or breathing cycle may also contribute to this scaling phenomenon since they may contaminate the Blood Oxygenated Level Dependent (BOLD) signal with properties depending on the sampling period of data (*i.e.,* short/long time of repetition (TR)) [3]. Early investigations therefore considered these space-varying low frequency components as noise, which are responsible for potential non stationarities. Hence, to fulfill the assumptions underlying the classical GLM implementation, most neuropsychologist resort to high-pass filtering to remove these trends. In the last few years, the GLM estimation method has been extended to account for $1/f$ (or fractional Gaussian) noise using wavelet decomposition [4].

However, other authors have pointed out that the BOLD signal itself contains power at virtually all frequencies, notably in randomized event-related designs [5]. Interestingly, recent studies have reported that low-frequency spatial fluctuations in cortical BOLD signals may be indicative of synchronized long memory neuronal oscillations rather than merely noise [6, 7]. Concomitantly, greater persistence or higher predictability summarized in terms of scaling exponent has been found in patients with Alzheimer disease or with major depressive disorder, especially in brain regions implicated in the early stages of the degeneracy process [6, 8]. This confirms that high-pass filtering may potentially remove part of the signal of interest. A first attempt to identify stimulus-induced signal changes from scaling parameters has been proposed in [9]. These authors have developed a voxel-based exploratory multifractal (MF) analysis of fMRI time series relying on the continuous wavelet transform. Scale invariance is associated with the intuition that no characteristic frequency (or scale of time) can be singled out in the data within a wide range of frequencies. In the present contribution, we make use of a new scaling analysis, which replaces long memory models with multifractal ones and wavelet coefficients with wavelet Leaders, quantities that bring significant gains in estimation performance.

Irrespective of the retained approach, analysis of scaling implies studying long enough time series. In [9], the authors tested MF analysis on Echo Planar Imaging (EPI) fMRI data, which temporal resolution was decreased down to 200ms for partial brain volume acquisition to get up to 1500 time points. Here we resort to a new imaging technique, called 3D parallel localized Echo Volumar Imaging (EVI), recently validated on the human brain [10], which will be able to cover the whole brain at very high magnetic field (*e.g.,* 7.T). To date, this imaging procedure enables a very high temporal resolution (one volume every 225ms) and thus permits acquisition of a larger number of brain volumes in a given period of time (here 2210 scans), without requiring subsequent slice-timing correction. This offers the possibility to perform reliable scaling analyses. This paper therefore aims at exploring the benefit of this new Leader based MF analysis in combination with EVI brain images.

For ease of interpretation, we implemented a slow event-related paradigm which studies occipital responses to the presentation of alternative contrast checkerboard. However, this can be extended to more complex experiments aiming at studying cognitive systems.

2. DATA ACQUISITION

Echo-Volumar Imaging technique. The principle of EVI has been introduced in [11]. Faster than EPI, EVI allows 3D single-shot acquisition of whole volumes of interest at very high scanning rates. Nevertheless, this acquisition technique requires very high performances from the MR hardware and is also more sensitive to B_0 inhomogeneities because of long echo train durations. Thus, only a few attempts at using EVI in fMRI have been performed until now, focusing mainly on small and very anisotropic brain volumes [12,13]. Due to improved gradient hardware and magnet homogeneity, and especially to the application of parallel acquisition and reconstruction, we demonstrated the feasibility to acquire an important isotropic part of the brain with EVI, at usual fMRI spatial resolution, in about 200 ms [14]. As summarized in Fig. 1(a) « Localized Parallel EVI » relies on the use of outer volume suppression pulses and parallel acquisition with undersampling by a factor of 2 along two directions, in order to reduce the echo train durations. Consequently, an $80 \times 80 \times 100\text{mm}^3$ brain volume can be acquired in 225 ms, with a level of distorsions comparable to EPI. Parallel reconstruction was performed using a home-made 2D SENSE reconstruction algorithm, which also requires one sensitivity map for each of the coils. Detection of cerebral functional activation using localized parallel EVI has already been demonstrated, both in block and event-related cognitive paradigms [10]. The results of these studies are currently compared with conventional 2D EPI acquisition using the same paradigm. First results suggest that the BOLD contrast to noise could be more important in EVI than in EPI, due to difference in acquisition parameters and T_1 weightings. All experiments were performed on a 1,5 T GEHC scanner (40 mT/m, 150T/m/s slew rate gradient, 8 channel head coil array). EVI acquisitions have been performed using the following parameters: orientation= sagittal plane, TE/TR $= 40/225$ ms, flip angle (FA) $= 35°$, BW $= 62.5$ kHz, FOV $= 80\times80\times100$ mm^3, acquired/reconstructed matrices = $20\times10\times10/20\times20\times20$, echo train duration = 60.5 ms. Sensitivity maps: sagittal plane, TE/TR $= 10/500$ ms, FA = 30°, BW $= 62.5$ kHz, FOV $= 240\times240\times100$ mm^3, matrix $60\times60\times20$.

fMRI expriment. The five healthy subjects gave their written informed consent and this study was approved by a local ethical committee for biomedical research. Two sessions of a slow visual event-related paradigm were acquired for each subject. The stimulus was a black and white contrast reversing checkerboard with a 20-ms period, which appears during 80 ms, followed by a 24.67-ms rest period (ISI = 24.75 s). One session consisted of 20 trials of the stimulus. All series were corrected for subject motion with SPM2 (www.fil.ion.ucl.ac.uk). No spatial smoothing was performed. Response magnitudes for each voxel were estimated using a general linear model with a canonical Hemodynamic Response Function (HRF) and its first derivative as regressors. A Fisher (F) test was performed to assess significance. 3D superimpositions with anatomical data were obtained with Anatomist (http://brainvisa.info). As illustrated in Fig. 1(b) for one subject, activations were detected both in occipital cortex and cerebellum. Fig. 1(c) shows voxel-based HRF estimates that have been computed in voxels eliciting an activation from the raw time courses. These raw data were first corrected from low-frequency drifts, then smoothed using a temporal Gaussian kernel ($\sigma^2 = 1.5$ s) and finally, averaged over the stimulus repetitions.

3. SCALING AND MULTIFRACTAL ANALYSIS

Scaling: self-similarity and wavelets. Data is said to possess a scale invariance, or *scaling*, property when their analysis does not

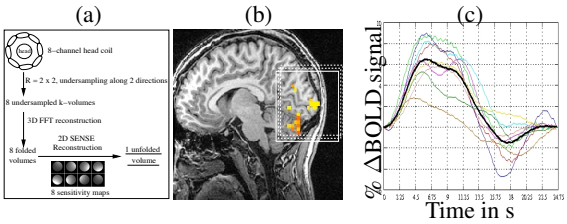

Fig. 1. (a): Sketch summarizing the Localized Parallel EVI sequence. (b): Localized volume acquired using the EVI sequence shown in white box and hot spots illustrating visual activations superimposed on anatomical data. (c): corresponding HRF estimates

enable the identification of any characteristic scale over a wide range of time scales. Equivalently, this means that all time scales are equally characteristic.

To analyze scale invariance, it is now commonly admitted that wavelet transforms constitute ideal tools [15]. Let $d_X(j,k) = \langle \psi_{j,k}, X \rangle$ denote the discrete wavelet transform coefficients of X, where $\psi_0(t)$ stands for the *mother-wavelet* and the $\{\psi_{j,k}(t) = 2^{-j}\psi_0(2^{-j}t-k)\}$ a collection of templates dilated and translated on the dyadic grid. The mother wavelet is characterized by a fast exponential decay and a strictly positive integer $N \geq 1$, the *number of vanishing moments*, defined as $\forall k = 0, 1, \ldots, N-1$, $\int_{\mathbb{R}} t^k \psi_0(t) dt \equiv 0$.

To model scale invariance, self-similarity (SS) provides us with a mathematically well-grounded framework. A process X is said to be self similar, with stationary increments, when it satisfies $\forall c > 0, \{X(t), t \in \mathbb{R}\} \stackrel{d}{=} \{c^H X(t/c), t \in \mathbb{R}\}$, where $\stackrel{d}{=}$ means equality of all finite dimensional distributions [16]. The SS parameter H is restricted to $H \in (0,1)$. The increments Y of X possess a $1/f$-spectrum: $\Gamma_Y(f) \simeq C|f|^{-\gamma}$ with $\gamma = 2H-1$. When $1/2 < H < 1$, Y is characterized by a long-range dependence property [16]. This explains why $1/f$ and long-range dependent processes are often incorrectly confused with the broader class of self-similar ones. In the wavelet framework, self-similarity implies that law behaviours hold, for all scales 2^j and all orders $q \in (-1, +\infty)$: $S^d(j,q) \stackrel{\Delta}{=} \frac{1}{n_j} \sum_{k=1}^{n_j} |d_X(j,k)|^q = C_q^d 2^{jqH}$ (with n_j the number of $d_X(j,k)$ at scale 2^j). Therefore, the logscale diagrams (LDs), $\log_2 S^d(j,q)$ *vs* $j = \log_2 2^j$, constitute central quantities for assessment of self-similarity (power-laws are turned into straight lines) and estimation of the parameter H (by linear regressions). Real fMRI data examples and the corresponding LDs are shown in Fig. 2.

Contribution. Both self-similar (and long range dependent) processes and wavelet tools have already been commonly used in the context of fMRI time series analysis [4, 6]. In the present work, we add two major stones. First, to model scaling, we use multifractal stochastic processes instead of self-similar ones, the major benefit being the versatility brought by the use of a collection of scaling exponents instead of the single self-similarity parameter H. Second, to analyze scaling, we replace wavelet coefficients by *wavelet Leaders*, which possess better theoretical properties for MF analysis [15] and those statistical estimation performance are improved by an order of magnitude (see *e.g.,* [17]).

Wavelet Leaders and Multifractal. In a nutshell, a wavelet Leader replaces a given wavelet coefficient by the largest wavelet coefficients existing in its (very) narrow time neighborhood at all finer scales $j' \leqslant j$. Technically, let $\psi_0(t)$ have compact support and let us define dyadic intervals as $\lambda = \lambda_{j,k} = \left[k2^j, (k+1)2^j\right)$ and $3\lambda = 3\lambda_{j,k} = \lambda_{j,k-1} \cup \lambda_{j,k} \cup \lambda_{j,k+1}$. Following [15], the wavelet Leaders are defined as: $L_X(j,k) \equiv L_\lambda = \sup_{\lambda' \subset 3\lambda} |d_{\lambda'}|$.

For the sake of simplicity, we only propose a practical introduction to multifractality. For a mathematical definition, the reader is referred

to [15]. A process X is said to be multifractal if, for a range of positive and negative statistical orders q and a range of scales $a = 2^j$, its structure functions $S^L(j,q)$ exhibit power law behaviours with respect to scales [15]:

$$S^L(j,q) \triangleq \frac{1}{n_j}\sum_{k=1}^{n_j} L_X(j,k)^q = C_q^L 2^{j\zeta(q)}. \quad (1)$$

The $\zeta(q)$ are referred to as the scaling exponents. They can be expanded as $\zeta(q) = \sum_{p=1}^{\infty} c_p \frac{q^p}{p!}$ where the c_p are defined from the cumulants of $\ln L_X(j,k)$(see [17]). For SS, $\zeta(q) = qH$, hence $c_1 = H$ and $\forall p \geq 2, c_p \equiv 0$. Therefore, the signature of MF lies in the departure of $\zeta(q)$ from a linear behaviour in q and hence mostly in $c_2 < 0$. In the present work, we restrict ourselves to the estimations of c_1 and c_2, hence to the approximation $\zeta(q) \simeq c_1 q + c_2 q^2/2$.

Practical wavelet Leader based multifractal (WLMF) analysis. Based on Eq. (1), the Leader logscale diagrams (LLD), $\log_2 S^L(j,q)$ *vs* $j = \log_2 2^j$, play key roles in assessing multifractal analysis and estimation. Examples are shown in Fig. 3. From the $L_X(j,k)$, a procedure, which has been fully developed and validated in [17], enables the estimation of the multifractal parameters c_1 and c_2.

4. RESULTS

Main issues. In the present work, the ensuing goal is twofold: First, validation of the existence of scaling in the analyzed data and estimation the MF parameters ; Second, differentiation of evoked from ongoing brain activity in terms of scaling behaviours. This has never been addressed in the fMRI literature using the WLMF approach. For doing so, we compare, by means of statistical hypothesis tests, MF parameters estimated from raw motion-corrected fMRI time series acquired during activation and resting runs from selected regions of interest (ROI). Importantly, these ROIs have been identified on each subject separately from the uniquely relevant F-contrast $c = [1, 1, 0]$ to detect activations in the above mentioned SPM2 analysis. The extracted SPM clusters have been corrected for multiple comparisons and thresholded below 5 % in corrected p-value and above 5 voxels in spatial extent. Note that the number of SPM clusters R varies from one subject to another.

Scaling Analysis. The first issue lies in assessing whether the data possess scaling or not. Using an adaptive representation, the *Empirical Mode Decomposition* (EMD) [18] applied to voxel-based time courses, we observe that the data can be split into 3 components (see Fig. 2(a)): a very low frequency trend (LF), a medium frequency signal (mF) and a high frequency noise (HF). Both the LF trend and the HF noise may either alter the analysis of scaling or be confusingly associated to scaling, as commonly speculated in the literature. However, the LDs computed from the original time series and from these 3 components, superimposed in Fig. 2(b), clearly show that the scaling property of interest is neither caused by the LF trend nor by the HF noise, but rather entirely due to the mF signal. It is worth noting that EMD is a data driven splitting procedure that hence avoids the recourse to any rigid a priori chosen high pass filter to remove non stationarities. Moreover, we checked that the LDs and estimated scaling parameters remain consistent when the number of vanishing moments of ψ_0 is varied. This observation is a strong empirical argument indicating the existence of true scaling and constitutes a major benefit of the wavelet scaling analysis framework. Therefore, the proposed procedure clearly disentangles true scaling properties from non stationary superimposed trends or high frequency noise corruption.

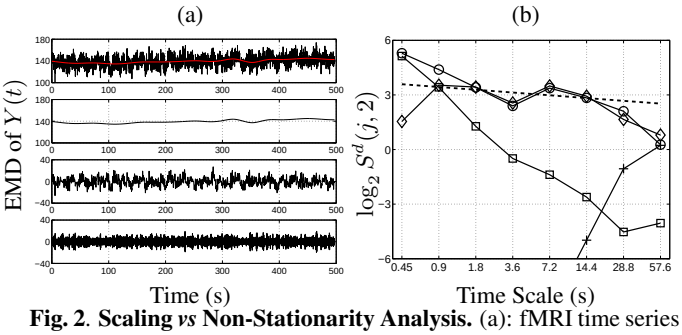

Fig. 2. **Scaling *vs* Non-Stationarity Analysis.** (a): fMRI time series for an activated voxel (subject 2), and its EMD based separation into (from top to bottom) low, medium and high frequency components. (b): the corresponding LDs (time series: 'o', LF: '+', mF: '$\diamond$', HF: '$\square$').

In a second step, we apply the WLMF analysis procedure to the voxel-based mF signal component for all voxels in the identified SPM clusters. The corresponding LLDs (*cf.* Fig. 3) yield clear scaling behaviours holding for $3 \leqslant j \leqslant 6$, i.e., for time scales ranging from 1.5 to 15s. A systematic voxel-based estimation of the multifractal parameters c_1 and c_2 can thus be conducted. For parameter c_1, we observe that it consistently takes values in the range $0.50 \leqslant c_1 \leqslant 1$ (cf. Table 1), both for on-going and evoked brain activity, hence confirming the relevance of the LRD paradigm to characterize fMRI time series correlations. Also, we note that activation systematically (for all subjects and all ROIs) results in an increase in c_1, from the range $0.50 \leqslant c_1 \leqslant 0.75$ for ongoing activity to the range $0.70 \leqslant c_1 \leqslant 0.95$ for evoked activity. Activation hence induces an increase of the LRD strength and impact. This is consistent with findings reported in [9]. For parameter c_2, the situation is more intricate as its estimation is by far more difficult [17]. However, we observe that, in most cases, activations coincide with an increase in c_2, from negative to close to 0 values, hence with a decrease in multifractality (cf. Table 1).

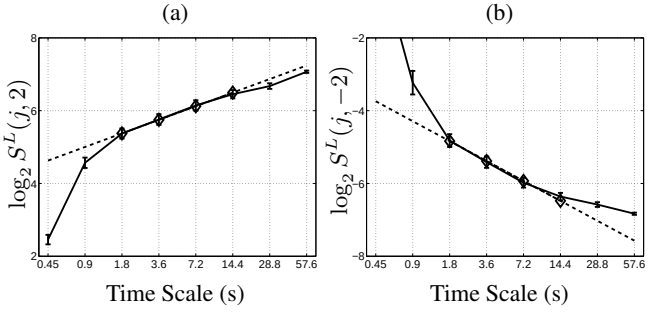

Fig. 3. **Leader based Multifractal Analysis.** LLDs for $q = 2$ (a) and $q = -2$ (b) show a clear scaling range, from 1.5 to 15s.

Region-based hypothesis testing. The next goal consists of assessing the statistical significance of the observed difference in every cluster R_i between $\mathrm{med}[\widehat{\boldsymbol{c}}_p^{\mathrm{r}}]$ and $\mathrm{med}[\widehat{\boldsymbol{c}}_p^{\mathrm{v}}]$. We use nonparametric tests and robust statistics as there is no evidence that the scaling parameters are normally distributed across voxels for a given ROI. In such a case, one usually resorts to robust decision statistics (*e.g.,* to the Wilcoxon's signed rank (WSR) statistic), whose correct specificity control (control of false positives) in the permutation testing framework has been developed in [19] on the basis of [20]. Here, robustness means that the influence of outliers on the statistics remains bounded. Precisely, we perform the following *two-sided* tests : $H_{0,p}^{\mathrm{r}\neq\mathrm{v}} : \mathrm{med}[\widehat{\boldsymbol{c}}_p^{\mathrm{r}}] = \mathrm{med}[\widehat{\boldsymbol{c}}_p^{\mathrm{v}}], \forall\ p = 1 \text{ or } 2$, which amounts to testing whether the difference between the matched samples $\widehat{\boldsymbol{c}}_p^{\mathrm{r}}$

	$\mathrm{med}[\hat{c}_1^{\mathrm{v}}]$	$\mathrm{med}[\hat{c}_2^{\mathrm{v}}]$	$\mathrm{med}[\hat{c}_1^{\mathrm{r}}]$	$\mathrm{med}[\hat{c}_2^{\mathrm{r}}]$	$H_{0,1}^{\mathrm{r}\neq\mathrm{v}}$	$H_{0,2}^{\mathrm{r}\neq\mathrm{v}}$
R_1^{Vis}	0.81 0.86	−0.005 0.098	0.69 0.55	−0.006 −0.038	0.019 0.125	0.966 0.125
R_2^{Vis}	0.89 0.75	−0.013 0.029	0.75 0.63	−0.019 −0.001	0.027 0.008	0.734 0.312
R_3^{Vis}	0.72 0.80	−0.02 0.068	0.66 0.70	−0.01 0.005	0.020 0.078	0.017 0.047

Table 1. **Median of the cumulant estimates and corresponding Wilcoxon's sign-rank tests**. The first column indicates the different SPM clusters. In each ROI, the columns provide the *median* of the voxel-dependent WLMF estimates $\widehat{c}_p^{\,s}$ for $p = 1 : 2$ and for visual (left $s = \mathrm{v}$) and rest (right, $s = \mathrm{r}$) sessions, for the second and third subjects, (top and bottom rows, respectively). The last two columns display the corresponding WSR statistic p-values. Red marks show significant changes at 5%. The number of voxels v_i embedded in R_i typically varies between 5 and 30 voxels.

and $\widehat{c}_p^{\,\mathrm{v}}$ comes from a distribution whose *median* $\mathrm{med}[\widehat{c}_p^{\,\mathrm{r}-\mathrm{v}}] = \mathrm{med}[\widehat{c}_p^{\,\mathrm{r}} - \widehat{c}_p^{\,\mathrm{v}}]$ is zero. The last two columns of Table 1 show the corresponding WSR statistic p-values and validate that the observed increase in c_1 is quasi-systematically significant. Again, for c_2, results are less clear, as significance of the changes varies with ROIs and subjects. However, results, over the entire data sets, that can not be shown here, indicate a shift tendency in c_2 form negative to close to 0 values, when the test is significant. This confirms a global effect of reduction of multifractality under activation.

To finish with, let us mention that we observe, in agreement with [17], that Leader based estimations outperform significantly wavelet coefficient ones. Notably, the confidence interval sizes for c_2 are decreased by one order of magnitude. This implies that WSR tests based on wavelet coefficients would miss a number of changes in c_1, despite their being net, and that it is strictly not possible to detect a change in c_2 using such coefficients. Relevant estimations of c_2 therefore constitute the major benefits of the use of Leaders.

5. CONCLUSIONS AND PERSPECTIVES

Making use of EVI fMRI data and of a slow event-related paradigm, we have shown that MF analysis based on wavelet Leaders enables to evidence changes under activation in fMRI time series scaling properties. Activation induces a clear increase in the self-similarity, which can be associated to random walks and linear filtering while multifractal is rather related to non-linear mechanisms. Therefore, parameter c_2 that characterizes deviations from SS can be thought as a measure of the importance of non-linear effects in neurophysiological mechanisms. Our results suggest that activation tends to reduce their impact: this could be expected given the very simple nature of our paradigm. Future work will investigate the ability to conduct MF analysis in more complex event-related designs with several stimulus types. In such cases, we could find out more multifractal situations, for instance in regions eliciting habituation or learning phenomena. Last but not least, we are currently exploring whole brain analysis blind to the use of any a priori model-based detection. We expect that MF parameters will be primarily influenced in brain regions involved in the experimental paradigm and also that these parameters remain unchanged in other regions when the comparing the activation dataset to the resting state one.

6. REFERENCES

[1] E. Zarahn et al., "Empirical analysis of BOLD fMRI statistics. I. Spatially unsmoothed data collected under null-hypothesis conditions," *Neuroimage*, vol. 5, pp. 179-, 1997.

[2] Ed. Bullmore et al., "Wavelets and functional MRI of the human brain," *Neuroimage*, vol. 23, pp. S234-, 2004.

[3] P. L. Purdon and R. M. Weisskoff, "Effect of temporal autocorrelation due to physiological noise and stimulus paradigm on voxel-level false-positive rates in fMRI.," *Hum. Brain Mapp.*, vol. 6(4), pp. 239-, 1998.

[4] J. Fadili and E. Bullmore, "Wavelet-generalized least squares: A new BLU estimator of linear regression models with 1/f errors," *Neuroimage*, vol. 15(1), pp. 217-, 2002.

[5] M. A. Burock et al., "Randomized event-related experimental designs allow for extremely rapid presentation rates using functional MRI.," *Neuroreport*, vol. 9(16), pp. 3735-, 1998.

[6] V. Maxim et al., "Fractional Gaussian noise, fMRI and Alzheimer's disease.," *Neuroimage*, vol. 25, pp. 141-, 2005.

[7] D. Leopold et al., "Very slow activity fluctuations in monkey visual cortex: implications for functional brain imaging.," *Cereb Cortex*, vol. 13(4), pp. 422-, 2003.

[8] K Linkenkaer-Hansen et al. "Breakdown of long-range temporal correlations in θ oscillations in patients with major depressive disorder.," *J Neurosci*, vol. 25(44), pp. 10131-, 2005.

[9] Yu Shimizu et al., "Wavelet-based multifractal analysis of fMRI time series.," *Neuroimage*, vol. 22, pp. 1195-, 2004.

[10] C. Rabrait et al., "Temporal analysis of the BOLD response using high temporal resolution Echo Volumar Imaging," in *Proc. 14th ISMRM*, 2006.

[11] P. Mansfield, "Multi-planar image formation using NMR spin-echoes," *J.Phys.C : Solid State Phys.*, vol. 10, pp. L55-, 1977.

[12] P. Mansfield et al., "Echo-volumar imaging (EVI) of the brain at 3T: first normal volunteer and functional imaging results," *J. Computer Assisted Tomography*, vol. 19, pp. 847-, 1995.

[13] W. van der Zwaag et al., "Echo volumar imaging (EVI) for high temporal resolution fMRI," in *Proc. 12th ISMRM*, Kyoto, Japan, 2004, p. 1005.

[14] C. Rabrait et al., "Development of a high temporal resolution echo-volumar imaging (EVI) sequence with outer volume saturation RF pulses, using SENSE reconstruction," in *Proc. 22th ESMRMB*, Basle, Switzerland, 2005.

[15] S. Jaffard et al., "Wavelet leaders in multifractal analysis," in *Wavelet Analysis and Applications,T Qian, M. I; Vai, X. Yuesheng, Eds.*, Basel, Switzerland, 2006, pp. 219-, Birkhäuser.

[16] G. Samorodnitsky and M. Taqqu, *Stable non-Gaussian random processes*, Chapman and Hall, New York, 1994.

[17] H. Wendt et al., "Bootstrap for log wavelet cumulant based multifractal analysis," in *EUSIPCO'06*, Firenze, Italy, 2006.

[18] N.E. Huang, et al. "The empirical mode decomposition and the hilbert spectrum for nonlinear and non-stationary time series analysis," *Proc. R. Soc. Lond. A*, vol. 454, pp. 903-, 1998.

[19] S. Mériaux et al., "Combined permutation test and mixed-effect model for group average analysis in fMRI.," *Hum. Brain Mapp.*, vol. 27, pp. 402-, 2006.

[20] T.E. Nichols and S. Hayasaka, "Controlling the Familywise Error Rate in Functional Neuroimaging: A Comparative Review," *Stat. Meth. in Med. Res.*, vol. 12, pp. 419-, 2003.